Biosensors and Bioelectronics 24 (2009) 1484–1489

Contents lists available at ScienceDirect

Biosensors and Bioelectronics

journal homepage: www.elsevier.com/locate/bios

Electrochemical detection of protein tyrosine kinase-catalysed phosphorylation using gold nanoparticles

Kagan Kerman, Heinz-Bernhard Kraatz*

Department of Chemistry, The University of Western Ontario, 1151 Richmond Street, London, Ont., Canada N6A 5B7

ARTICLE INFO

Article history:
Received 14 August 2008
Received in revised form 24 October 2008
Accepted 27 October 2008
Available online 6 November 2008

Keywords:
Electrochemical biosensor
Colloidal gold nanoparticles
Phosphorylation
Protein tyrosine kinase
Abl-T315I
Staurosporine

ABSTRACT

Protein tyrosine kinase (PTK)-catalysed phosphorylation reactions of peptides are monitored electrochemically in the presence of Au nanoparticles (NPs) on peptide modified indium tin-oxide (ITO) electrodes. The method is based on the thiophosphorylation using adenosine 5′-[γ-thio] triphosphate (ATP-S) as the co-substrate. Upon thiophosphorylation of the peptides, the Au NPs accumulate on the surface and can be detected electrochemically by monitoring Cl^- oxidation at the Au NP surface. The activity of a clinically important PTK, Abl-T315I, which is implicated in the therapy of chronic myelogenous leukaemia (CML), is determined. Abl-T315I was assayed in combination with its highly specific substrate peptide EGI**Y**DVP. The detection limit for the electrochemical detection of Abl-T315I activity was 10 ng/mL. The performance of the biosensor was optimized and control experiment using non-specific peptide-modified electrodes were carried out. The electrochemical current response obtained from the Cl^- oxidation chemistry enabled monitoring the inhibition of the thiophosphorylation reactions using staurosporine, a small molecule inhibitor.

1. Introduction

Human genome sequence analysis has identified about 518 human protein kinases, constituting about 1.7% of all the human genes (Robinson et al., 2000). Within this large "kinome", at least 90 tyrosine kinase genes have been identified, 58 of which are receptor tyrosine kinases (RTKs) and 32 non-receptor tyrosine kinases (NRTKs). A significant number of protein tyrosine kinases (PTKs, both receptor and non-receptor types) are associated with cancers (Schlessinger, 2000). Clinical studies suggest that overexpression/de-regulation of PTKs may be of prognostic/predictive value in patients and may indicate aggressive tumour biology or may predict poor response to therapy and shorter survival (Hunter, 1998). PTKs play a central role in oncogenic transformation of cells (Blume-Jensen and Hunter, 2001).

During PTK-catalysed phosphorylation, the γ-phosphoryl of ATP is transferred to specific tyrosine residues of the protein (Cohen, 2002a,b). Thus, modifications on the γ-position of ATP provided a novel trend of detection methods. Recently, Elphick et al. (2007) reviewed the approaches on the design of ATP analogues and protein kinase binding site mutants. In particular, adenosine 5′-[γ-biotin] triphosphate (ATP-biotin) has been utilized in phophorylation assays as a promising alternative to the existing technologies (Green and Pflum, 2007; Kerman et al., 2007a). Wang et al. (2005, 2006) utilized the optical properties of Au nanoparticles (NPs) and developed kinase activity assays in connection with ATP-biotin. Recently, Oishi et al. (2007) developed a colorimetric kinase-activity evaluation method utilizing cationic substrate peptides as potential coagulants of citrate-coated Au NPs with anionic surface charge. Allen et al. (2007) and Blethrow et al. (2008) utilized adenosine 5′-[γ-thio] triphosphate (ATP-S) to create an epitope for thiophosphate-ester specific antibodies. In our group, we also utilized ATP-S for the electrochemical detection of phosphorylation of a target peptide catalysed by protein kinase C, a serine-threonine kinase (Kerman and Kraatz, 2007). Our group has also demonstrated the use of adenosine 5′-[γ-ferrocene] triphosphate (ATP-Fc) as an electro-active co-substrate for the kinase-catalysed phosphorylation reactions (Song et al., 2008). In a label-free format, field-effect transistor-based detection of kinase activity was developed by Freeman et al. (2007). Kerman et al. (2007b) have also reported a label-free method to determine small molecule inhibitors of PTKs using the electrochemical oxidation of tyrosine residues in substrate peptides.

The routinely used tools to detect phosphorylation involve mass spectroscopy (Steen et al., 2005; Kruger et al., 2006), radioisotopes (Houseman et al., 2002; Turk et al., 2006; Hastie et al., 2006) and fluorescent labels (Sato et al., 2002; Umezawa, 2005; Tomizaki and Mihara, 2006), phospho-specific antibodies in connection with surface plasmon resonance (Stenlund et al., 2006; Catimel et al., 2006;

* Corresponding author. Tel.: +1 519 661 2111x81561; fax: +1 519 6613022.
E-mail address: hkraatz@uwo.ca (H.-B. Kraatz).

0956-5663/$ – see front matter © 2008 Elsevier B.V. All rights reserved.
doi:10.1016/j.bios.2008.10.024

Viht et al., 2007) and fluorescence-based systems (Allen et al., 2006; Rothman et al., 2005; Shults et al., 2005; Han et al., 2008).

In this work, we present our results describing an electrochemical biosensor for the detection of PTK activity using Abl1-T315I as the model enzyme. The method is based on the labelling of a specific thiophosphorylation reaction of substrate peptides with ATP-S and Au NPs, followed by electrochemical detection using the Cl^- redox chemistry. Briefly, the biotinylated PTK substrate peptides were immobilized on streptavidin-coated indium-tin oxide (ITO) electrode surface. After PTK-catalysed thiophosphorylation, the peptide surface was exposed to Au NPs (20 nm, A_{525} = 0.5). The electrochemical response obtained from the Cl^- on Au NPs enabled monitoring the activity and inhibition of Abl-T315I *in vitro*.

2. Experimental

2.1. Reagents

Colloidal Au NPs (20 nm) were purchased from Sigma. The purified recombinant Abl1-T315I mutant, as well as its biotinylated substrate peptide, biotin-EGI**Y**DVP were purchased from Cell Signalling Technology (MA, USA). Streptavidin from *Streptomyces avidinii*, (3-aminopropyl)triethoxysilane (APTES) and biotinamidohexanoic acid *N*-hydroxysuccinimide ester (biotin-NHS) were purchased from Sigma–Aldrich. Other reagents were purchased from Merck and Sigma–Aldrich. All solutions were prepared and diluted using ultra-pure water (18.3 MΩ cm) from the Millipore MilliQ system.

2.2. Instruments

Square wave voltammetry (SWV) was performed using a CHInstruments 660 system (Austin, TX). Indium-tin oxide (ITO) coated glass substrates (resistivity between 8 and 12 Ω) were used as the working electrode and were purchased from Structure Probe, Inc. (West Chester, PA).

2.3. Procedure

2.3.1. Electrode pre-treatment

The electrode pre-treatment was carried out before the surface modifications with the aim of improving the sensitivity and reproducibility of the results. Briefly, ITO electrodes were immersed into acetonitrile, isopropanol and methanol solutions, respectively and sonicated for 5 min in each solution. The electrodes were washed extensively using MilliQ after each sonication process.

2.3.2. Immobilization of the biotinylated substrate peptides on streptavidin-modified ITO electrodes

The substrates were subsequently immersed in a 10% (v/v) aqueous solution of APTES as the amino-functional silane for 2 h. From our research, this concentration of APTES solution and immersion time was enough to deposit sufficient APTES on the substrate. After immersion, the substrates were dipped in MilliQ to rinse off excess APTES for 30 min. MilliQ was slowly and continuously added to the beaker and overflowed to prevent deposition of other substances present on the water surface, when the substrate was removed from the water. The substrate was then dried in air for 10 min. After drying, the substrate was baked at 120 °C for 10 min in a glass jar that was pre-heated on a hot plate, and its temperature was monitored using a thermometer. This baking time was found enough to prevent elution of APTES from the sufficiently rinsed substrate (data not shown). After the APTES-modified ITO electrode is brought back to room temperature, an aliquot of 10 μM biotin-NHS solution (100 μL) in 0.1 M MES (pH 6) was dropped on the surface and the covalent modification of the surface was allowed for 2 h (Fig. 1). After a stringent washing of the surface to remove excess biotin-NHS, an aliquot of 10 μM streptavidin solution (100 μL) was allowed to coat the working electrode of the biotin-modified ITO electrodes and kept overnight at 4 °C. Free surface sites of the streptavidin-modified ITO electrodes were blocked with 1.0% (w/v) Tween-20 in MilliQ. Then, the biotinylated peptides were immobilised by incubating for 90 min on the streptavidin-coated surface. After this incubation step, the peptide-modified ITO electrodes were rinsed with MilliQ.

2.3.3. Abl1-T315I-catalysed phosphorylation

The activity of Abl1-T315I kinase was measured using the following conditions: 60 mM HEPES (pH 7.5), 5 mM $MgCl_2$, 5 mM $MnCl_2$, 3 μM Na_3VO_4, 200 μM ATP-S in a total reaction volume of 100 μL. The peptide-modified ITO electrodes were incubated at 37 °C for 2 h in a block-heater. The reaction solution (100 μL) was used to cover the whole peptide-modified surface. After rinsing the electrodes with MilliQ water, the peptide-modified surface was covered with 100 μL Au NP solution (20 nm, A_{525} = 0.5) and incubated at room temperature for 30 min. After rinsing the electrodes with MilliQ water, the electrodes were used for the electrochemical measurements.

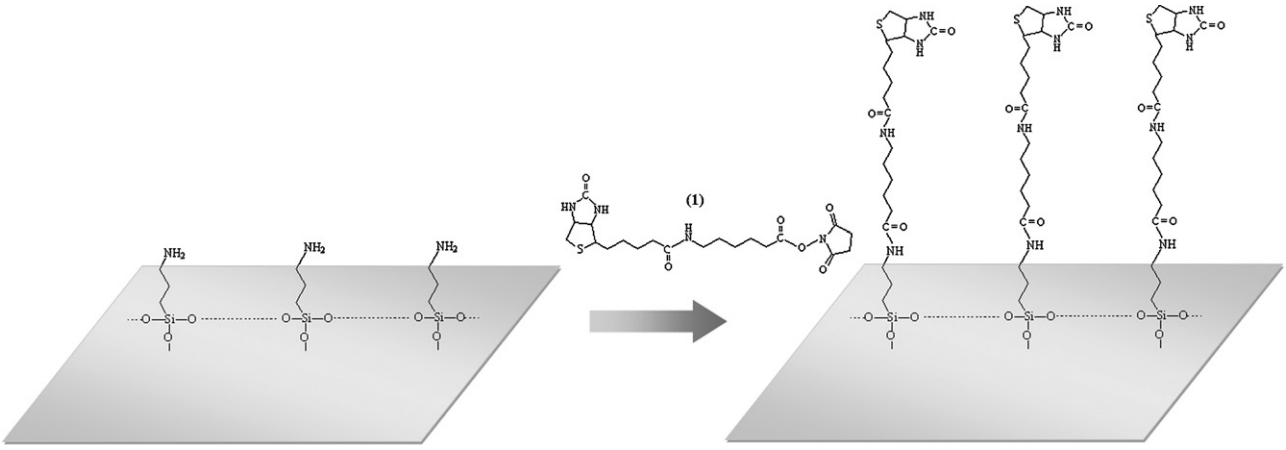

Fig. 1. Biotinylation of the APTES-modified ITO electrodes using biotinamidohexanoic acid *N*-hydroxysuccinimide ester (1). The APTES-modified electrodes were exposed to (1) for 2 h in 0.1 M MES (pH 6).

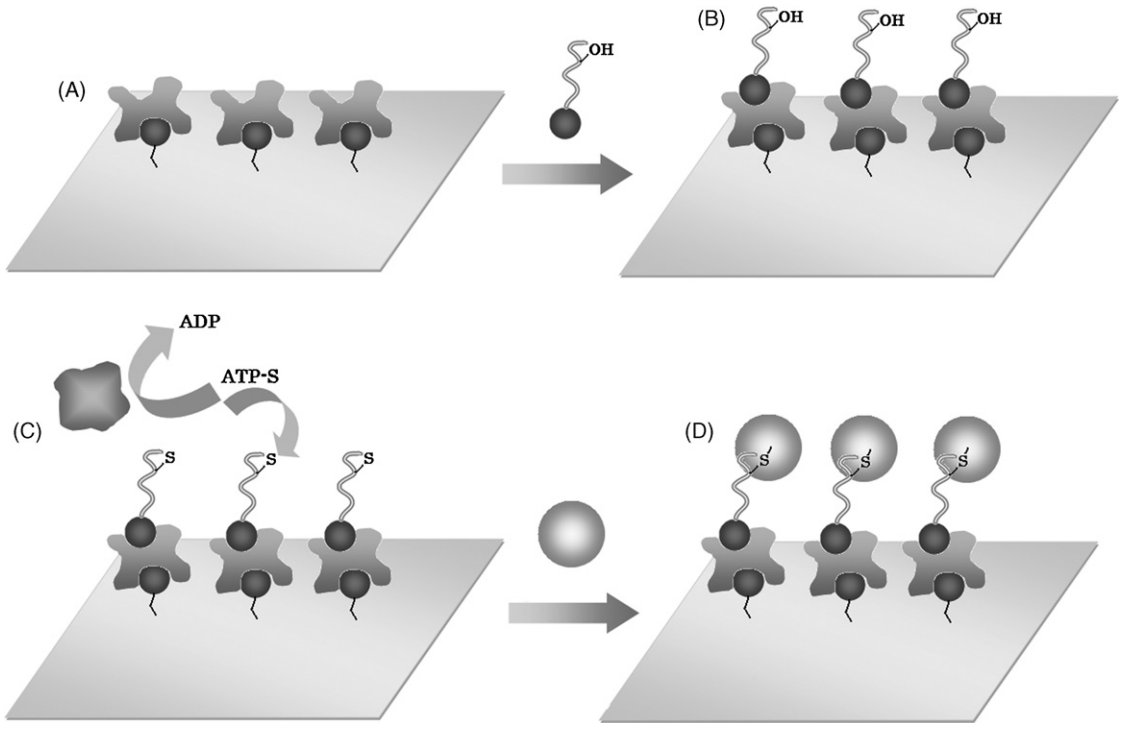

Fig. 2. The experimental flow-chart of the Au nanoparticle-based detection of kinase-catalysed phosphorylation reactions on the ITO electrodes. Biotin-modified ITO electrodes (A) are modified with streptavidin to enable the attachment of the biotinylated peptides on the surface (B). The protein tyrosine kinase (PTK)-catalysed phosphorylation reaction transfers the γ-thiophosphate group from ATP-S to the substrate peptides (C) resulting in the formation of ADP. The exposure of the thiolated peptides to Au NPs results in their accumulation on the surface (D).

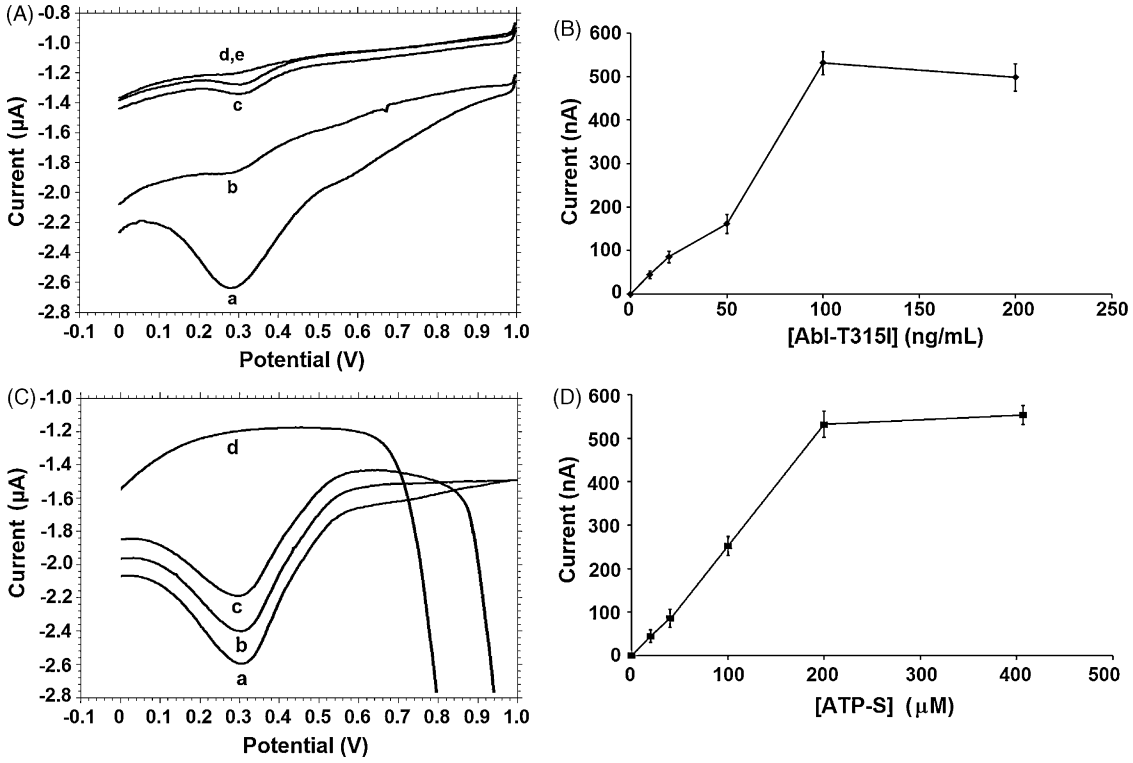

Fig. 3. (A) Square-wave voltammograms for the electrochemical detection of Abl-T315I-catalysed phosphorylation reactions on peptide (biotin-EGI**Y**DVP) modified ITO electrodes. The reduction peak at 0.3 V showed dependence on the amount of the kinase involved in the reaction, (a) 100 ng/mL, (b) 20 ng/mL, (c) 10 ng/mL, (d) 5 ng/mL, and (e) no enzyme in the reaction buffer (60 mM HEPES (pH 7.5), 5 mM $MgCl_2$, 5 mM $MnCl_2$, 3 μM Na_3VO_4, 200 μM ATP-S). (B) Plot for the dependence of current signals on the Abl-T315I concentration in the phosphorylation reactions. The electrochemical measurements were performed for three times at each condition ($n = 3$), except otherwise stated. The data points show the average of three measurements with the error bars indicating the relative standard deviation (R.S.D.). (C) square-wave voltammograms for the detection of optimum ATP-S concentration for the Abl-T315I-catalysed phosphorylation reactions on peptide (biotin-EGI**Y**DVP). The reduction signal showed dependence on the amount of the co-factor ATP-S, (a) 400 μM, (b) 200 μM, (c) 150 μM, (d) no ATP-S. (D) plot for the dependence of current signals on the ATP-S concentration in the phosphorylation reactions ($n = 3$). The data points show the average of three measurements with the error bars indicating the R.S.D.

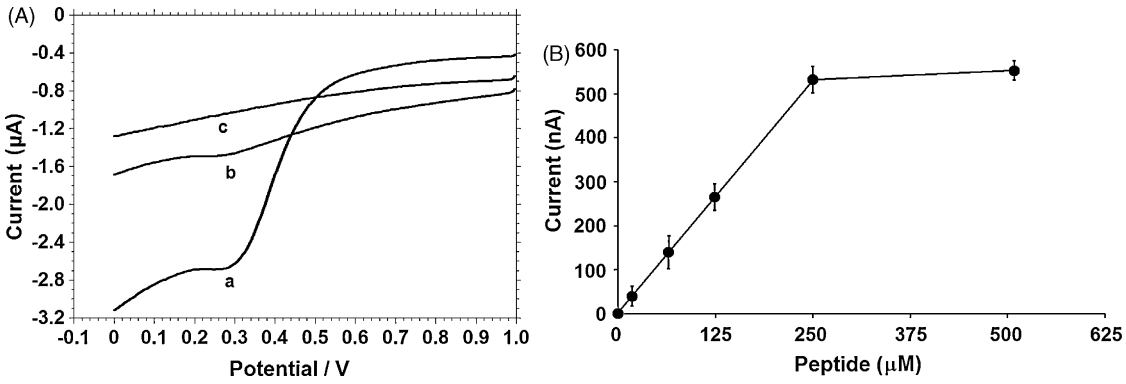

Fig. 4. (A) Square-wave voltammograms for the electrochemical detection of Abl-T315I-catalysed (50 ng/mL) phosphorylation reactions on peptide-modified ITO electrodes. The reduction signal showed dependence on the amount of the immobilized peptides involved in the reaction: (a) 250 μM, (b) 25 μM, (c) no peptides on the ITO electrode. Other experimental conditions were as described in Fig. 3. (B) Plot for the dependence of current signals on the peptide concentration in the phosphorylation reactions ($n = 3$). The data points show the average of three measurements with the error bars indicating the R.S.D.

2.3.4. Electrochemical measurement on ITO surface

Electrochemical experiments were carried out in an in-house made cell specifically designed for flat working electrodes (Khan et al., 2008). After filling the cell with 0.1 M HCl (pH 2, 5 mL), reference electrode (Ag/AgCl) and the counter electrode (Pt wire) were inserted into the solution. Square wave voltammetry (SWV) involved the oxidation of Au NPs by applying 1.20 V for 60 s. Immediately after this oxidation procedure, the oxidized ions were reduced by sweeping the potential from 1 to 0 V with an amplitude of 25 mV at 15 Hz frequency.

3. Results and discussion

The experimental flow-chart is shown in Fig. 2 for the electrochemical detection of PTK-catalysed phosphorylation reactions on the ITO surface using Au NPs. The biotinylated substrate peptides were attached o the streptavidin-coated surface. The enzymatic reaction took place under controlled temperature in a block-heater. After the reaction, the electrodes were washed and the thiophosphorylated peptides were exposed to Au NPs. After rinsing the electrodes, the surface-attached Au NPs were detected using a single-surface redox process, which involved the oxidation of the Au NPs at 1.2 V for 1 min in 0.1 M HCl (pH 2). As a result of this oxidation step in highly acidic environment, $[AuCl_4]^-$ ions were produced and the biomolecules were denaturated on the surface. The denaturation of biomolecules allowed a large electrode surface for the $[AuCl_4]^-$ ions to be reduced back at ~0.4 V (vs. Ag/AgCl). The voltammetric detection of Au NPs via the Cl^- chemistry on a single surface has recently been reported as a simple and highly sensitive detection method for DNA hybridization and antibody-antigen interactions (Pumera et al., 2005a,b; Kerman et al., 2007a,b; Idegami et al., 2008).

Fig. 3A shows the SWV responses obtained from the reduction scans from 1 to 0 V (vs. Ag/AgCl) following the Abl-T315I-catalysed phosphorylation reactions. The concentrations of substrate peptide and ATP-S were kept constant at 250 and 200 μM, respectively. The dependence of the current responses on Abl-T315I concentration was recorded as shown in Fig. 3B. The peak current heights reached a saturation level, when Abl-T315I concentrations reached over 100 ng/mL. The detection limit for the phosphorylation activity of Abl-T315I on peptide modified ITO surface was determined as 10 ng/mL.

In order to optimize the experimental conditions, a series of measurements were taken in the presence of varying ATP-S concentrations and 100 ng/mL Abl-T315I as shown in Fig. 3C. When 200 μM ATP-S was used together with 100 ng/mL Abl-T315I, a high current response was observed (Fig. 3C-b) indicating that the surface-immobilized substrate peptides were phosphorylated efficiently. As the concentration of ATP-S increased, the phosphorylation of the peptides resulted in the increased accumulation of Au NPs on the surface (Fig. 3D). The current responses did not increase significantly for concentrations over 200 μM (Fig. 3C-a), thus, 200 μM ATP-S was applied for further assays. In the absence of ATP-S, no significant current response was observed indicating negligible non-specific adsorption of Au NPs (Fig. 3C-d). The voltammograms and plot for the detection of HER2, which is an important target in the breast cancer therapy, are presented in the Supplementary data section.

As shown in Fig. 4A, the current responses were also dependent on the amount of peptides that were immobilized on the ITO surfaces. By using 200 μM ATP-S and 100 ng/mL Abl-T315I, the concentration of the peptides immobilized on the surface was varied between 25 μM (Fig. 4A-b) and 250 μM (Fig. 4A-a). As a control experiment, we performed the same PTK assay on a different substrate peptide, which cannot be phosphorylated by Abl-T315I (biotin-SIYRRG**S**RRWRKL). This control peptide contained a Ser residue, which was specifically designed for phosphorylation by protein kinase C (PKC). When the ITO surface was coated with 250 μM of the control peptide, negligible current responses were observed indicating the non-specifically bound Au NPs could not be detected on the surface (Fig. 4A-c). Fig. 4B shows a plot describing the influence of peptide concentration on the electrochemical current response. A linear range for the peptide concentration was observed between 10 and 500 μM with five experimental data

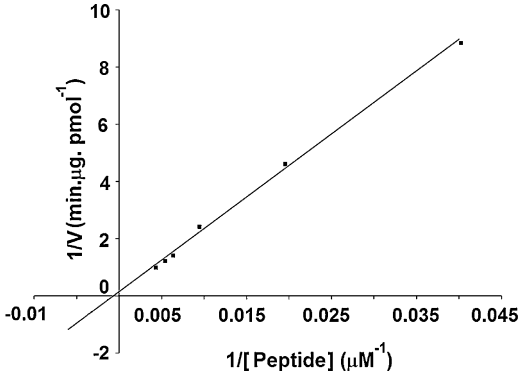

Fig. 5. Lineweaver–Burk plot for the determination of kinetics of the Abl1-T315I-catalysed phosphorylation of the immobilized substrate peptide at varying surface density conditions on the Au microelectrode surface.

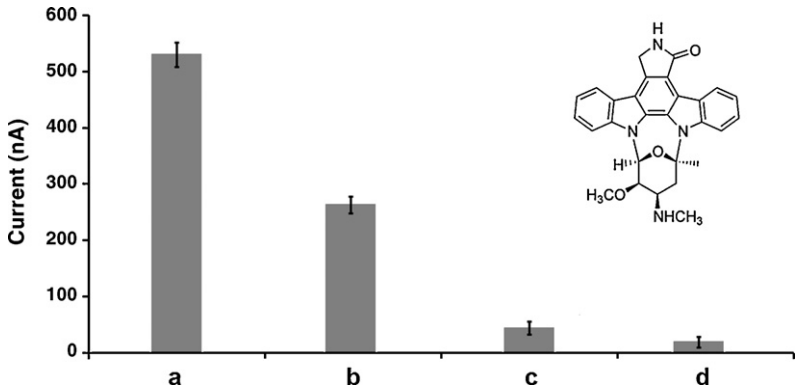

Fig. 6. Plot for the dependence of current responses on the concentration of the general protein kinase inhibitor staurosporine: (a) no inhibitor, (b) 0.5 μM, (c) 1 μM, (d) 2 μM. As the concentration of staurosporine increased in the reaction buffer including 200 ng/mL Abl-T315I, the amount of Au NPs attached on the surface decreased, leading to a decrease in the current signals ($n = 3$). Experimental conditions were as described in Fig. 3 except the addition of the inhibitor in the reaction buffers.

points. For each concentration the reaction was carried out in triplicate with three measurements for each concentration in order to get statistically meaningful data. The paired and unpaired *t*-test between the results obtained from target peptides and non-target peptides indicated the two-tailed *P* values less than 0.005, which was considered to be statistically significant with the confidence interval of 95%. For the results obtained from four measurements using 250 μM target peptide-modified electrode, the Chi-squared equalled 1.388 with the two-tailed *P* value of 0.71, thus, the difference between these measurements was not considered to be statistically significant. Moreover, the paired and unpaired t-test between the two sets of four measurements using 250 μM target peptide-modified electrode indicated the two-tailed *P* values between 0.14 and 0.23, which was not considered to be statistically significant with the confidence interval of 95%.

The time dependence of the phosphorylation reactions was determined by stopping the reaction at different time intervals and measuring the current response (data not shown). A saturation level in the signals was reached after 2 h incubation in the presence of 100 ng/mL Abl-T315I. When the reaction was stopped at 150 min, no significant increase in the reduction peak responses was observed. For the determination of the phosphorylation kinetics, measurements were performed in which the surface concentrations of the peptide were varied. The initial time dependence of the kinase reactions was determined at varying peptide density conditions. The phosphorylation reaction was stopped after 5, 15, 30, 60, 90, 120 and 150 min, and the electrochemical measurement was carried out after each time interval. The reciprocals of these current values were plotted against the reciprocal of the peptide density, giving linear Lineweaver–Burk plot (Fig. 5). The kinetic data extracted from the Lineweaver–Burk plot are given in Table 1. The K_m value was in agreement with the literature values determined using radioactive labelling techniques (Houseman et al., 2002; Turk et al., 2006; Hastie et al., 2006).

Staurosporine is an ATP-competitive inhibitor with broad-spectrum inhibitory activities. For Abl, the K_i value for staurosporine determined by radio-labelling systems is 620 nM (Weisberg et al., 2007; Carter et al., 2005). Fig. 6 shows the current response for the inhibition of the Abl-T315I-catalysed thiophosphorylation reactions as a function of staurosporine concentration. Addition of 500 nM of staurosporine to the measurement solution causes the current response to drop by 50% (Fig. 6b). The current responses dropped to negligible values, when more than 1 μM staurosporine was added to the assay buffer (Fig. 6c and d). This concentration range, in which the inhibitory effects of staurosporine were observed, was in agreement with the reported literature (Weisberg et al., 2007; Carter et al., 2005; Tikhomirov and Carpenter, 2001).

Table 1
Kinetic constants of Abl1-T315I with its substrate peptide immobilized on ITO electrodes.

Protein kinase	Peptide	K_m (mM)	V_{max} (pmol min^{-1} μg^{-1})	V_{max}/K_{max}
Abl1-T315I	EGIYDVP	0.672	6.73	10.02

4. Concluding remarks

Our electrochemical studies demonstrate the use of Au NPs and ATP-S in PTK reactions on surface-immobilized substrate peptides. The experimental conditions were optimized using Au NPs as the electro-active indicator. The Cl^- redox chemistry on a single surface was utilized to detect the activity and inhibition of Abl-T315I, which is implicated in CML. The electrochemical biosensor reported here is promising for further development toward *in vitro* electrochemical kinase profiling and inhibitor screening studies. Biosensors will have important implications on the development of high-throughput and multiplexed nanoparticle-based kinase assays for the screening of small molecule kinase inhibitors as promising anti-cancer drugs. The success of our inhibition measurements in this paper indicate clearly that the electro-activity of Cl^- in the presence of Au NPs is potentially a useful alternative method of determining small molecule inhibitors of kinases and that this approach versatile and can tolerate a wide range of transducer surfaces and kinases. With the current success of small molecule kinase inhibitors in cancer therapy, our electrochemical results reported here pave the way to the development of a rapid screening tool for drug candidates, which will undoubtedly have potential applications in pharmaceutical research.

Acknowledgements

K. K. acknowledges the post-doctoral fellowship from the Ontario Ministry of Research and Innovation. The authors are grateful to Professor D. W. Litchfield at the University of Western Ontario for his kind donations of chemical reagents and experimental facilities.

Appendix A. Supplementary data

Supplementary data associated with this article can be found at doi:10.1016/j.bios.2008.10.024.

References

Allen, M.D., DiPilato, L.M., Rahdar, M., Ren, Y.R., Chong, C., Liu, J.O., Zhang, J., 2006. ACS Chem. Biol. 1, 371–376.

Allen, J.J., Li, M., Brinkworth, C.S., Paulson, J.L., Wang, D., Hubner, A., Chou, W.-H., Davis, R.J., Burlingame, A.L., Messing, R.O., Katayama, C.D., Hedrick, S.M., Shokat, K.M., 2007. Nat. Methods 4, 511–516.

Blethrow, J.D., Glavy, J.S., Morgan, D.O., Shokat, K.M., 2008. Proc. Natl. Acad. Sci. USA 105, 1442–1447.

Blume-Jensen, P., Hunter, T., 2001. Nature 41, 355–365.

Carter, T.A., Wodicka, L.M., Shah, N.P., Velasco, A.M., Fabian, M.A., Treiber, D.K., Milanov, Z.V., Atteridge, C.E., Biggs III, W.H., Edeen, P.T., Floyd, M., Ford, J.M., Grozfeld, R.M., Herrgard, S., Insko, D.E., Mehta, S.A., Patel, H.K., Pao, W., Sawyers, C.L., Varmus, H., Zarrinkar, P.P., Lockhart, D.J., 2005. Proc. Natl. Acad. Sci. USA 102, 11011–11016.

Catimel, B., Layton, M., Church, N., Ross, J., Condron, M., Faux, M., Simpson, R.J., Burges, A.W., Nice, E.C., 2006. Anal. Biochem. 357, 277–288.

Cohen, P., 2002a. Nat. Rev. Drug Discov. 1, 309–315.

Cohen, P., 2002b. Nat. Cell Biol. 4, E127–E130.

Elphick, L.M., Lee, S.E., Gouverneur, V., Mann, D.J., 2007. ACS Chem. Biol. 2, 299–314.

Freeman, R., Gill, R., Willner, I., 2007. Chem. Commun., 3450–3452.

Green, K.D., Pflum, M.K.H., 2007. J. Am. Chem. Soc. 129, 10–11.

Han, X., Shigaki, S., Yamaji, T., Yamanouchi, G., Mori, T., Niidome, T., Katayama, Y., 2008. Anal. Biochem. 372, 106–115.

Hastie, C.J., McLauchlan, H.J., Cohen, P., 2006. Nat. Protoc. 1, 968–971.

Houseman, B.T., Huh, J.H., Kron, S.J., Mrkisch, M., 2002. Nat. Biotechnol. 20, 270–274.

Hunter, T., 1998. Philos. Trans. Biol. Sci. 353, 583–605.

Idegami, K., Chikae, M., Kerman, K., Nagatani, N., Yuhi, T., Endo, T., Tamiya, E., 2008. Electroanalysis 20, 14–21.

Kerman, K., Kraatz, H.-B., 2007. Chem. Commun., 5019–5021.

Kerman, K., Chikae, M., Yamamura, S., Tamiya, E., 2007a. Anal. Chim. Acta 588, 26–33.

Kerman, K., Vestergaard, M., Tamiya, E., 2007b. Anal. Chem. 79, 6881–6885.

Khan, M.A.K., Kerman, K., Petryk, M., Kraatz, H.-B., 2008. Anal. Chem. 80, 2574–2582.

Kruger, R., Kubler, D., Pallisse, R., Burkovski, A., Lehmann, W.D., 2006. Anal. Chem. 78, 1987–1994.

Oishi, J., Asami, Y., Mori, T., Kang, J.-H., Tanabe, M., Niidome, T., Katayama, Y., 2007. ChemBioChem 8, 875–879.

Pumera, M., Aldavert, M., Mills, C., Merkoçi, A., Alegret, S., 2005a. Electrochim. Acta 50, 3702–3707.

Pumera, M., Castaneda, M.T., Pividori, M.I., Eritja, R., Merkoçi, A., Alegret, S., 2005b. Langmuir 21, 9625–9629.

Robinson, D.R., Wu, Y.M., Lin, S.F., 2000. Oncogene 19, 5548–5557.

Rothman, D.M., Shults, M.D., Imperiali, B., 2005. Trends Cell Biol. 15, 502–510.

Sato, M., Ozawa, T., Inukai, K., Asano, T., Umezawa, Y., 2002. Nat. Biotechnol. 20, 287–294.

Schlessinger, J., 2000. Cell 103, 211–225.

Shults, M.D., Janes, K.A., Lauffenburger, D.A., Imperiali, B., 2005. Nat. Methods 2, 277–283.

Song, H., Kerman, K., Kraatz, H.-B., 2008. Chem. Commun., 502–504.

Steen, H., Jebanathirajah, J.A., Springer, M., Kirschner, M.W., 2005. Proc. Natl. Acad. Sci. USA 102, 3948–3953.

Stenlund, P., Frostell-Karlsson, A., Karlsson, O.P., 2006. Anal. Biochem. 353, 217–225.

Tikhomirov, O., Carpenter, G., 2001. J. Biol. Chem. 276, 33675–33680.

Tomizaki, K., Mihara, H., 2006. Mol. Biosyst. 2, 580–589.

Turk, B.E., Hutti, J.E., Cantley, L.C., 2006. Nat. Protoc. 1, 375–379.

Umezawa, Y., 2005. Biosens. Bioelectron. 20, 2504–2511.

Viht, K., Schweinsberg, S., Lust, M., Vaasa, A., Raidaru, G., Lavogina, D., Uri, A., Herberg, F.W., 2007. Anal. Biochem. 362, 268–277.

Wang, Z., Lee, J., Cossins, A.R., Brust, M., 2005. Anal. Chem. 77, 5770–5774.

Wang, Z., Levy, R., Fernig, D.G., Brust, M., 2006. J. Am. Chem. Soc. 128, 2214–2215.

Weisberg, E., Manley, P.W., Cowan-Jacob, S.W., Hochhaus, A., Griffin, J.D., 2007. Nat. Rev. Cancer 7, 345–356.